Phenotypic analysis of misato function reveals roles of noncentrosomal microtubules in Drosophila spindle formation.

Violaine Mottier-Pavie, Giovanni Cenci, Fiammetta Vernì, Maurizio Gatti, Silvia Bonaccorsi

Phenotypic analysis of *misato* function reveals roles of noncentrosomal microtubules in *Drosophila* spindle formation

Violaine Mottier-Pavie[1,*], Giovanni Cenci[2], Fiammetta Vernì[1], Maurizio Gatti[1] and Silvia Bonaccorsi[1,‡]

[1]Istituto Pasteur-Fondazione Cenci Bolognetti and Istituto di Biologia e Patologia Molecolari del CNR, Dipartimento di Genetica e Biologia Molecolare, "Sapienza" Università di Roma, Ple. A. Moro 5, 00185 Roma, Italy
[2]Dipartimento di Biologia di Base ed Applicata, Università dell'Aquila; 67010 Coppito, L'Aquila, Italy
*Present address: Department of Pharmacology, University of Texas Southwestern Medical Center, Dallas, TX 75390-9051, USA
‡Author for correspondence (silvia.bonaccorsi@uniroma1.it)

Accepted 21 October 2010
Journal of Cell Science 124, 706-717

doi:10.1242/jcs.072348

Summary

Mitotic spindle assembly in centrosome-containing cells relies on two main microtubule (MT) nucleation pathways, one based on centrosomes and the other on chromosomes. However, the relative role of these pathways is not well defined. In *Drosophila*, mutants without centrosomes can form functional anastral spindles and survive to adulthood. Here we show that mutations in the *Drosophila misato* (*mst*) gene inhibit kinetochore-driven MT growth, lead to the formation of monopolar spindles and cause larval lethality. In most prophase cells of *mst* mutant brains, asters are well separated, but collapse with progression of mitosis, suggesting that k-fibers are essential for maintenance of aster separation and spindle bipolarity. Analysis of *mst*; *Sas-4* double mutants showed that mitotic cells lacking both the centrosomes and the *mst* function form polarized MT arrays that resemble monopolar spindles. MT regrowth experiments after cold exposure revealed that in *mst*; *Sas-4* metaphase cells MTs regrow from several sites, which eventually coalesce to form a single polarized MT array. By contrast, in *Sas-4* single mutants, chromosome-driven MT regrowth mostly produced robust bipolar spindles. Collectively, these results indicate that kinetochore-driven MT formation is an essential process for proper spindle assembly in *Drosophila* somatic cells.

Key words: Spindle assembly, Monopolar spindles, Microtubule growth, Mitosis, *Drosophila*

Introduction

To form a mitotic spindle, centrosome-containing cells exploit microtubules (MTs) nucleated by the centrosomes, MTs nucleated in the vicinity of the chromosomes and MTs nucleated at the cell periphery or within the spindle. Most of these MTs are nucleated by the γ-tubulin ring complexes (γ-TuRCs), which are either embedded into the centrosome or free in the cytoplasm (reviewed by Lüders and Stearns, 2007; O'Connell and Khodjakov, 2007; Walczak and Heald, 2008).

In animal somatic cells, centrosomes are the major MT-organizing centers (MTOCs). They consist of a pair of centrioles surrounded by pericentriolar material (PCM), a proteinaceous meshwork that harbors the γ-TuRCs, which promote MT nucleation (reviewed by Bettencourt-Dias and Glover, 2007). Classic work by Kirschner and Mitchinson postulated that spindle morphogenesis is driven by dynamic centrosome-nucleated MTs, which 'search' the cytoplasm for chromosomes until they are captured and stabilized by the kinetochores (Kirschner and Mitchison, 1986). However, subsequent studies showed that centrosome-containing cells can exploit MTs nucleated near the chromosomes to assemble functional bipolar spindles in the absence of MTs nucleated by the centrosomes (Basto et al., 2006; Bonaccorsi et al., 2000; Khodjakov et al., 2000; Megraw et al., 2001). Whether astral MTs are present or not, kinetochores drive the formation of MT bundles that eventually give rise to the k-fibers that connect the kinetochores with the spindle poles. It has been suggested that the plus ends of chromatin-induced MTs are captured by the kinetochores and continue to polymerize there, leading to growing bundles of MTs with minus ends that are pushed away from the kinetochores (Lüders et al., 2006; Maiato et al., 2004b). These kinetochore-driven k-fibers are not initially oriented towards the spindle poles. However, as they grow, they are captured by the astral MTs, become connected with the spindle poles, and are integrated into a bipolar spindle (Maiato et al., 2004b).

Formation of chromosome-dependent MTs involves the GTP-bound form of Ran GTPase, which is generated in the vicinity of chromosomes by RCC1, a chromosome-associated Ran-GTP exchange factor. In mammalian cells, Ran-GTP regulates several MT-associated proteins that are required for MT stability, including Aurora A, TPX2 (targeting protein for Xklp2), NuMA (nuclear mitotic apparatus protein 1), HURP (hepatoma upregulated protein, also known as DAP-5), Aurora B, INCENP (inner centromere protein), Msps/XMAP215 and Nup107-160 (reviewed by Ciciarello et al., 2007; Kalab and Heald, 2008; Mishra et al., 2010). Consistent with these findings, depletion of TPX2, HURP, Aurora B, INCENP or Nup107-160 impairs chromosome-dependent MT formation, leading to severely defective mitotic spindles (Casanova et al., 2008; Kallio et al., 2002; Mishra et al., 2010; Sampath et al., 2004; Tulu et al., 2006).

Recent work has suggested that additional MTs can be nucleated by γ-TuRCs that associate laterally with pre-existing spindle MTs, leading to spindle amplification (Goshima et al., 2008; Mahoney et al., 2006; Zhu et al., 2008). It has been proposed that in *Drosophila* S2 cells, γ-TuRCs are anchored to the spindle MTs by

Journal of Cell Science

augmin, a multiprotein complex that contains at least nine subunits (Goshima et al., 2008; Meireles et al., 2009; Wainman et al., 2009). However, additional studies in *Drosophila* S2 cells have shown that the function of augmin is not limited to MT-based MT generation within the spindle. Augmin interacts with the Ndc80–Nuf2 and TACC (transforming acidic coiled-coil protein)–Msps complexes and is required for kinetochore-driven MT formation and k-fiber assembly (Bucciarelli et al., 2009). An augmin-related multiprotein complex has also been identified in human cells (Lawo et al., 2009; Uehara et al., 2009). Disruption of human augmin results in a variety of mitotic defects, including centrosome fragmentation, destabilization of kinetochore microtubules and defective chromosome segregation (Lawo et al., 2009; Uehara et al., 2009; Zhu et al., 2008).

Spindle MTs can also originate from secondary MT-organizing centers (sMTOCs) independently of both centrosomes and chromosomes. For example, in centrosome-free mouse oocytes, the spindle self-organizes from multiple γ-tubulin-enriched sMTOCs that nucleate MTs during prophase and then congress at the center of the cells to form a bipolar spindle (Gueth-Hallonet et al., 1993; Palacios et al., 1993; Schuh and Ellenberg, 2007). These sMTOCs form astral MT arrays even in chromosome-free oocyte fragments, indicating that sMTOCs form asters by MT nucleation and not by capture of MTs nucleated near the chromosomes. γ-tubulin-enriched sMTOCs have been also observed in acentriolar *Drosophila* tissue culture cells. These sMTOCs and their associated MTs contribute to spindle pole assembly, and also mediate de novo MT formation during anaphase and telophase (Moutinho-Pereira et al., 2009). Finally, there is evidence that MT bundles nucleated near the remnants of the nuclear envelope but far from both the chromosomes and the centrosomes contribute to spindle assembly in *Drosophila* spermatocytes (Rebollo et al., 2004).

Collectively, these results indicate that several pathways contribute to the formation of spindle MTs. However, the relative contributions of these pathways to spindle assembly and functioning are poorly defined. Here, we describe the role of the *misato* (*mst*) gene in *Drosophila* spindle assembly. We show that *mst* mutant spindles are often monopolar and exhibit low MT density. In addition, our results indicate that *mst* is required for kinetochore-driven MT growth, and that *mst* mutant cells fail to satisfy the spindle checkpoint and remain arrested in metaphase. *mst* mutants die at late larval stages with severely defective imaginal discs and relatively small brains, indicating a strong defect in cell proliferation (Gatti and Goldberg, 1991). Thus, the chromosome-dependent MT nucleation pathway is essential for *Drosophila* spindle formation, and to allow development to adulthood.

Results

The *Drosophila misato* (*mst*) gene encodes a 574 amino acid protein; the Mst N-terminal part contains motifs found in α-, β- and γ-tubulins, bacterial Ftsz, as well as a coiled-coil motif similar to that in myosin heavy chain (Miklos et al., 1998) (Fig. 1A). The Mst protein is conserved from yeast to humans and it has been implicated in the control of mitochondria distribution and fusion (Gurvitz et al., 2002; Kimura and Okano, 2007). We sequenced two *mst* alleles: mst^{C27} and mst^{LB20}. The X-ray-induced mst^{C27}

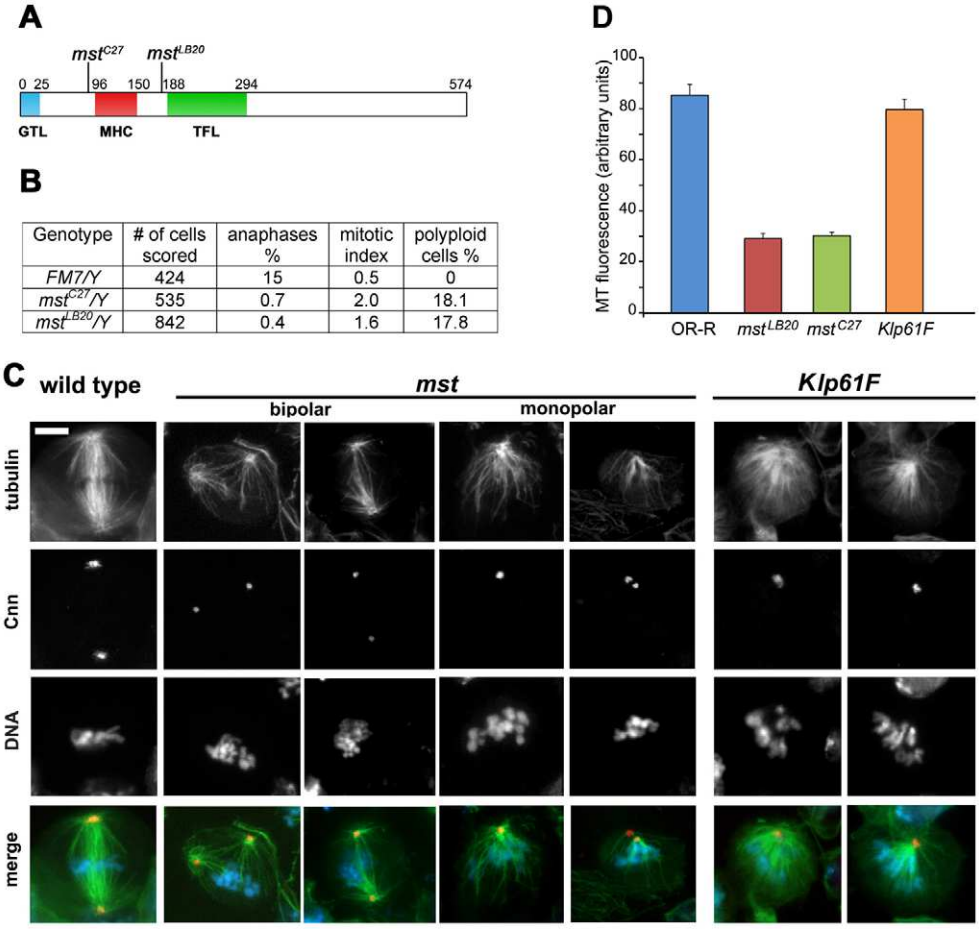

Fig. 1. Mutations in *mst* disrupt bipolar spindle formation. (**A**) Molecular map of the Mst protein showing the γ-tubulin-like (GTL), the myosin heavy chain-like (MHL), and the tubulin and Ftsz-like (TFL) domains. The position of the stop codons associated with the *mst* mutant alleles are indicated by vertical lines. (**B**) Mitotic parameters in larval brains from *mst* mutants. *FM7/Y* are control males bearing the *FM7* balancer chromosome. (**C**) Wild-type, *mst* and *klp61F* neuroblast metaphases stained for centrosomin (Cnn, red), tubulin (green) and DNA (blue). Note that the *klp61F* monopolar spindles exhibit a higher MT density than their *mst* counterparts. Scale bar: 5 µm. (**D**) MT fluorescence intensity of wild-type (OR-R) half spindles and monopolar spindles from *mst* and *Klp61F* mutants. Error bars indicate s.e.m.

allele carries an 11 base pair deletion (from nucleotide 175 to 185) leading to a stop codon that truncates the Mst protein to an 89 amino acid peptide. The EMS-induced mst^{LB20} allele contains a C-T transvection at nucleotide 544, which generates a stop codon leading to a truncated protein of 181 amino acids (Fig. 1A). These findings along with a western blotting analysis of Mst expression (see below) strongly suggest that the two *mst* alleles are genetically null.

Mst is required for bipolar spindle formation

mst mutations have been associated with a strong mitotic defect that causes reduction of the imaginal disk tissues, polyploid cells in larval brains and late larval lethality (Miklos et al., 1998). Our analysis of DAPI-stained brain preparations from mst^{C27}/Y and mst^{LB20}/Y larvae revealed that both mutant alleles produce a metaphase arrest phenotype, characterized by a high mitotic index, extremely condensed metaphase chromosomes, the almost complete absence of anaphases and an elevated frequency of polyploid cells (Fig. 1B).

Drosophila brains contain mainly two types of cells: neuroblasts and ganglion mother cells (GMCs). Neuroblasts are stem cells that undergo repeated asymmetric divisions that generate another neuroblast and a smaller GMC. Neuroblast metaphases exhibit centrosomes and asters of similar sizes at the two cell poles (Fig. 1C). However, with progression through anaphase and telophase, the MTs of the basal aster shorten dramatically, whereas those of the apical aster elongate slightly. By contrast, GMCs display equally-sized centrosomes and very small asters throughout mitosis; they divide symmetrically only once, giving rise to neurons or glial cells (Bonaccorsi et al., 2000). To determine the primary defect caused by *mst* mutations, we examined brain preparations stained for α-tubulin, DNA and centrosomin (Cnn), which is a core component of the pericentriolar material (PCM) required for astral MT nucleation (Li and Kaufman, 1996; Megraw et al., 2001). Strikingly, both mst^{C27} and mst^{LB20} neuroblasts showed an extremely high frequency of monopolar spindles [72% (n=500) and 76% (n=212), respectively]. Most of these aberrant spindles displayed two clear centrosomal signals at the spindle pole, suggesting a defect in centrosome separation. Interestingly, although some monopolar spindles had abnormally long MTs, other displayed short MTs (Fig. 1C). Most spindles with long MTs were associated with normally condensed chromosomes (83%, n=46), whereas most of those with short MTs (82%, n=37) displayed overcondensed chromosomes. Because chromosome overcondensation is a typical consequence of a metaphase block, these results strongly suggest that a prolonged metaphase arrest results in MT shortening. Morphologically abnormal spindles were also observed in mutant GMCs, which showed 69% (n=52) monopolar spindles (not shown).

Most spindles observed in *mst* mutants showed a lower MT density than metaphase spindles of wild-type cells. To estimate MT density, we measured MT fluorescence of *mst* monopolar spindles and wild-type half spindles of comparable size. In addition, we compared the MT fluorescence of monopolar spindles from *mst* and *Klp61F* mutants. KLP61F/Eg5 is a kinesin that is required for bipolar spindle formation; *Klp61F* mutants exhibit high frequencies of both monopolar spindles and polyploid cells (Heck et al., 1993). We found that the monopolar spindles from *mst* mutants displayed a lower MT density than either wild-type half spindles or *klp61F* nonopolar spindles (Fig. 1D). Thus, the low MT density observed in most *mst* spindles is not a general consequence of spindle monopolarity, but is specifically related to the loss of the *mst* function.

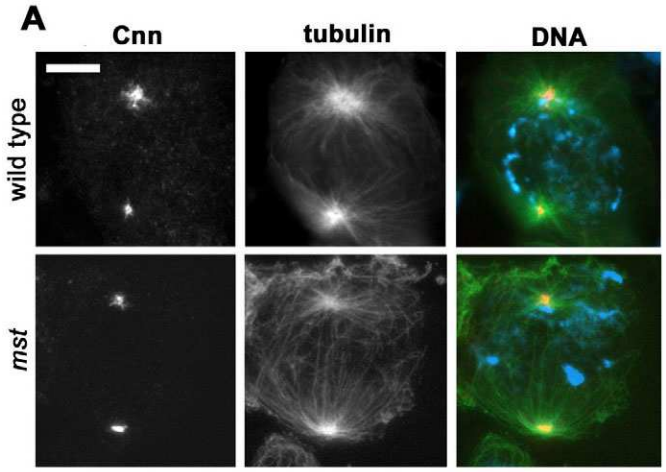

B

Genotype	Mitotic phase	# of cells	Cells showing the indicated angle (%)		
			<90°	90°-135°	136°-180°
FM7/Y	prophase	49	14	41	45
mst^{C27}/Y	prophase	30	23	40	37
FM7/Y	metaphase	250	0	12	88
mst^{C27}/Y	metaphase	243	65	5	30

Fig. 2. *mst* monopolar spindles are generated by aster collapse. (**A**) Wild-type and *mst* neuroblast early prophases stained for centrosomin (Cnn, red), tubulin (green) and DNA (blue). Note that in both the wild-type and the mutant prophase figures the centrosomes are localized at the opposite sides of the nucleus. Scale bar: 5 μm. (**B**) Centrosome localization in dividing neuroblasts from wild-type (bearing the *FM7* balancer) and *mst* mutant brains. To evaluate the position of the centrosomes relative to the prophase nucleus, we measured the angle between the two lines that connect the centre of the nucleus with the centrosomes.

We next investigated the mechanism underlying defective centrosome separation in *mst* mutants. Recent studies have demonstrated that the centrioles of *Drosophila* neuroblasts separate during interphase. Following cell division, one centriole remains stationary at the neuroblast apical cortex; the second centriole moves throughout the cell until, shortly before mitosis, it localizes at the neuroblast basal pole. As a consequence, the two centrosomes of wild-type neuroblasts are already well separated in early prophase and form asters at the opposite sides of the nucleus (Rebollo et al., 2007; Rusan and Peifer, 2007) (Fig. 2). To determine whether the monopolar spindles observed in *mst* brains are due to a failure in centrosome separation during interphase, we compared centrosome localization in early neuroblast prophases from wild-type and *mst* brains. Most mutant prophases displayed distant centrosomes, separated by angles comparable with those observed in wild-type prophases (Fig. 2). These findings strongly suggest that in *mst* mutant cells the centrosomes separate normally during interphase but then collapse during mitosis, leading to monopolar spindles.

Because *mst* mutants are characterized by centrosome misbehavior and aberrant arrays of astral MTs, we also investigated the role of *mst* in centrosome assembly and maturation. We asked whether the *mst* wild-type function is required for proper

localization of centrosome-associated proteins with known roles in centrosome structure and/or function. We analyzed the distribution of Sas-4, which is essential for centriole replication; γ-tubulin and Dd4/grip91 (γ-tubulin complex component 3 homolog), which have roles in astral MT nucleation; Cp309/PLP, Cnn and Spd-2 (spindle-defective protein 2), which are involved in centrosome maturation and MT nucleation; and TACC, which forms a complex with the mini spindles protein (Msps) and stabilizes centrosomal MTs (reviewed by Bettencourt-Dias and Glover, 2007; Giansanti et al., 2008). All these antigens regularly accumulated at the poles of both monopolar and bipolar spindles of *mst* mutant brains (supplementary material Fig. S1), indicating that Mst is not essential for their recruitment at the centrosomes.

mst mutant cells fail to satisfy the spindle assembly checkpoint

In bipolar metaphases of *mst* mutant brains, chromosomes were rarely aligned on a metaphase plate and robust kinetochore MT (kMTs) bundles were often absent. These phenotypic features suggest that mutant cells do not satisfy the spindle assembly checkpoint (SAC). To test this hypothesis, we immunostained *mst* brains for Zw10, a component of the Rod–Zw10–Zwilch (RZZ) complex, which is known to have a crucial role in SAC activity (reviewed by Karess, 2005). In *mst* brains immunostained for Zw10, strong kinetochore signals were consistently detected in 96% of metaphase cells (n=124). In addition, Zw10 remained associated with the kinetochores in all bipolar cells (n=35), and was never redistributed along the kMTs as occurs in most (67%, n=60) wild-type metaphases (Fig. 3A) (Karess, 2005; Williams et al., 1992). Collectively, these results indicate that in the arrested metaphases of *mst* mutants the SAC is not satisfied.

SAC activity explains why bipolar *mst* metaphases fail to enter anaphase. However, the question remained of whether the residual kMTs present in these cells can mediate chromosome segregation. We thus examined brain preparations from *mst; rod* double mutants, where the SAC is constitutively inactive. These double mutants showed a frequency of ana-telophases that was significantly higher than that observed in *mst* single mutants (Fig. 3B,C). In addition, the ana-telophases of the *mst; rod* double mutants displayed chromosome segregation defects much more severe than those seen in *rod* single mutants (Fig. 3B). These results indicate that the kMTs of *mst* bipolar cells retain at least a partial ability of driving anaphase chromosome movement.

Misato is required for kinetochore-driven MT formation

We next asked whether the low MT density observed in *mst* mutant spindles is the consequence of a reduced kinetochore-driven MT formation. To address this question, we performed a spindle microtubule regrowth assay in prometaphases and metaphases following cold-induced MT depolymerization. In wild-type cells, after 40 minutes of cold treatment, MTs were completely depolymerized and no longer detectable, with the exception of an array of very short MTs associated with the centrosomes (Fig. 4A). After return to room temperature for 1 minute, MT regrowth foci were primarily associated with the pericentric regions of the chromosomes and not with chromosome arms (Fig. 4A and data not shown). This finding strongly suggests that these foci are MT bundles emanating from kinetochores, which is consistent with studies in S2 cells showing that initial MT regrowth after cold exposure is tightly associated with the kinetochores (Bucciarelli et al., 2009). After 2 minutes at room temperature, most neuroblasts

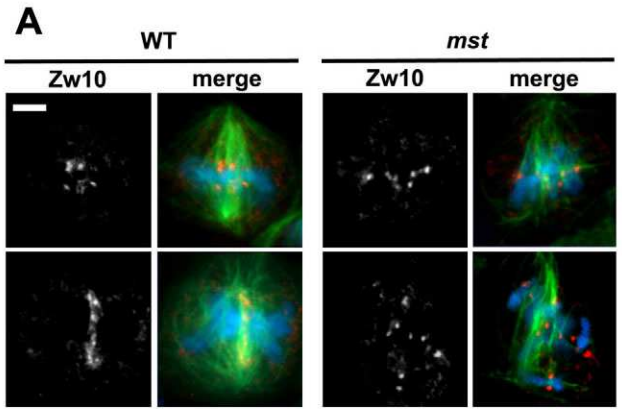

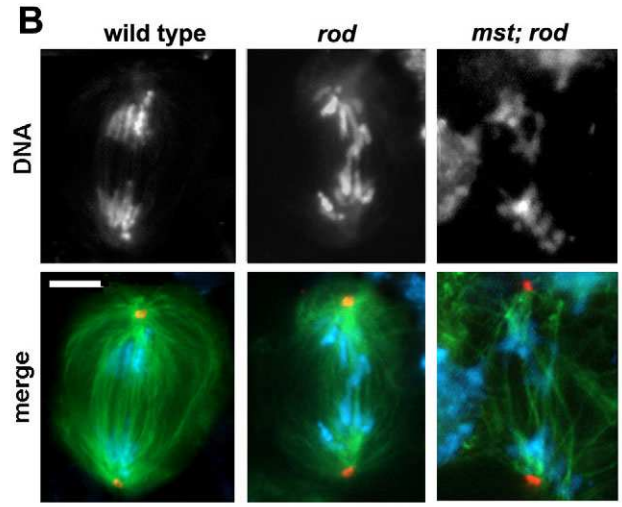

C

Genotype	# of mitotic figures	Anaphases %	Polyploid cells %
mst^{LB20}	460	1.1*	21.3
mst^{LB20}/rod^{1100}	308	7.8*	12.0

Fig. 3. *mst* mutant cells do not satisfy the spindle checkpoint. (**A**) Wild-type and *mst* neuroblast metaphases stained for Zw10 (red), tubulin (green) and DNA (blue). In wild-type neuroblasts, Zw10 consistently redistributes along kMTs during late metaphase (left panel; bottom row); in *mst* mutant cells Zw10 is never released from kinetochores. Scale bar: 5 µm. (**B**) Anaphase figures from wild-type, *rod* and *mst; rod* brains stained for centrosomin (Cnn, red), tubulin (green) and DNA (blue). Scale bar: 5 µm. (**C**) Frequency of anaphases observed in *mst* mutants and *mst; rod* double mutants. Note that the metaphase arrest phenotype of *mst* mutants is alleviated by mutations in *rod*; *P<0.001 (χ^2 test).

displayed prominent MT arrays associated with either the chromosomes or both the chromosomes and the centrosomes. After 5 minutes, the kinetochore-driven k-fibers and centrosomal MTs were incorporated into a typical metaphase spindle**,** in which the MT density was comparable with that observed before depolymerization (Fig. 4A,B).

The MT regrowth pattern observed in *Drosophila* neuroblasts is at odds with observations in mammalian systems, where initial MT regrowth following chemical or cold-induced MT depolymerization occurs at both the kinetochores and the centrosomes (De Brabander

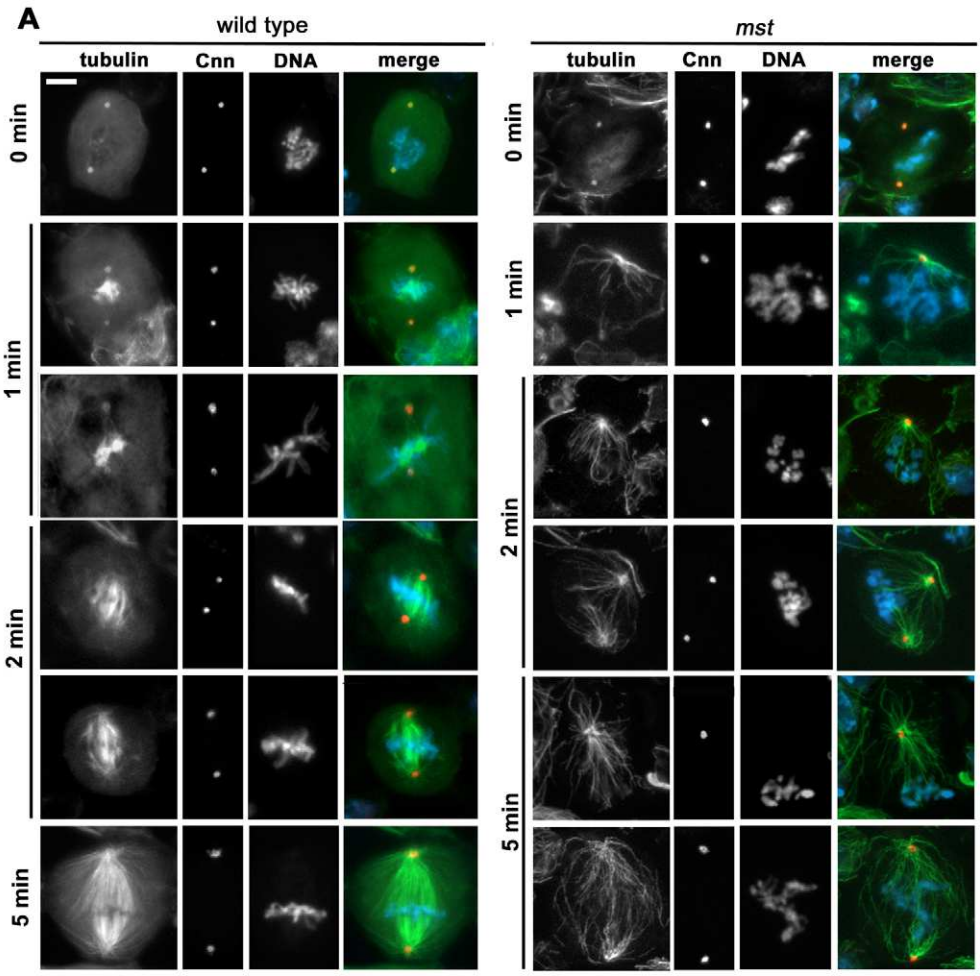

B

Genotype, time	# of cells	ch %	cn %	ch, cn %
wt, 1 min.	50	65	0	35
wt, 2 min.	37	47	0	53
wt, 5 min.	30	0	0	100

C

Genotype, time	# of cells	ch %	cn %	ch, cn %
mst, 1 min.	37	0	100	0
mst, 2 min.	51	0	96	4
mst, 5 min.	36	0	97	3

Fig. 4. Mst is required for chromosome-driven MT growth. (**A**) MT regrowth after cold depolymerization in wild-type and *mst* neuroblast metaphases. Cells were stained for centrosomin (Cnn, red), tubulin (green) and DNA (blue). In both wild-type and *mst* brains, spindle MTs are completely depolymerized after 40 minutes of cold treatment, except for some very short centrosome-associated MTs (0 minutes). In wild-type cells, MT repolymerization occurs exclusively near the chromosomes, or at both the chromosomes and the centrosomes (1 and 2 minutes); at 5 minutes, most spindles exhibit a normal morphology. In *mst* cells, no MT nucleation near the chromatin is observed at any time; at 5 minutes, *mst* spindles exhibit abnormally long centrosome-nucleated MTs. Scale bar, 5 μm. (**B**,**C**) Frequencies of wild-type (B) and *mst* (C) metaphases showing MT nucleation from the chromosomes only (ch), from the centrosomes only (cn), or from both the chromosomes and the centrosomes (ch, cn).

et al., 1981; Lüders et al., 2006; Tulu et al., 2006; Witt et al., 1980). However, our findings are in good agreement with previous observations on *Drosophila* S2 cells, where after either colcemid or cold treatment, formation of kinetochore-associated MT bundles precedes MT regrowth from the centrosomes (Bucciarelli et al., 2009; Goshima et al., 2008). Thus, *Drosophila* kinetochores and centrosomes appear to differ from their mammalian counterparts in their relative abilities to drive MT regrowth.

Cold treatment for 40 minutes also induced a complete spindle MT depolymerization in *mst* mitotic cells, here again with the only exception of some very short centrosome-associated MTs. However, after 1 minute at room temperature, *mst* prometaphases and metaphases were strikingly different from their wild-type counterparts. These mutant cells displayed substantial MT growth from the centrosomes but did not show kinetochore-associated MT bundles. The same pattern of MT regrowth was observed after 2 minutes at room temperature. In these cells, however, the MTs emanating from the centrosomes were longer than after 1 minute of regrowth, and in a few cases contacted the kinetochores. After 5 minutes at room temperature, *mst* monopolar and bipolar metaphase figures displayed very long centrosome-nucleated MTs that were often captured by the kinetochores, but did not show MTs that appeared to be nucleated around the chromosomes (Fig. 4A,C). We suggested above that the monopolar spindles with short MTs observed in *mst* brains are the consequence a prolonged metaphase arrest. The finding that all cold-exposed monopolar cells returned to room temperature for 5 minutes exhibited very long centrosomal MTs fully supports this conclusion.

An analysis of prophases returned to room temperature for 1 minute, revealed that *mst* centrosomes nucleated astral MTs, similarly to their wild-type counterparts (Fig. 5). Because chromatin cannot induce MT formation during prophase because of the presence of the nuclear envelope, this finding suggests that the different patterns of MT regrowth observed in wild-type and mutant cells do not reflect functional differences in centrosome activity. Thus, the most likely explanation for our observations is that chromosome- and centrosome-associated γ-TuRCs (reviewed by Lüders and Stearns, 2007) compete for the tubulin heterodimers required for MT polymerization, leading to overgrowth of asters in the absence of kinetochore-driven MT formation (Bucciarelli et

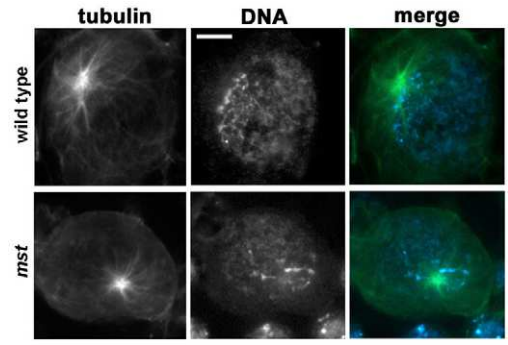

Fig. 5. MT regrowth in cold-treated wild-type and *mst* prophases returned to 25°C for 1 minute. Wild-type and mutant cells display comparable patterns of centrosome-driven MT regrowth. Scale bar, 5 μm.

al., 2009; Tulu et al., 2006). This hypothesis would also explain why the MTs nucleated by the centrosomes of *mst* mutant cells are longer than their wild-type counterparts. Collectively, our MT regrowth experiments strongly suggest that *mst* mitotic cells are primarily defective in kinetochore-driven MT formation.

We next tested whether the *mst* kinetochores have the ability to recruit selected components of the kinetochore machinery (Maiato et al., 2004a; Przewloka et al., 2007; Schittenhelm et al., 2007). Immunostaining for Cid/Cenp-A, Cenp-C, Ndc80/Hec1, Ial/Aurora B, Incenp or Cenp-meta/Cenp-E revealed that all these proteins bind the kinetochores of *mst* chromosomes (supplementary material Fig. S2 and data not shown). These findings indicate that the *mst* function is not required for proper localization of essential kinetochore proteins.

Spindle assembly in centrosome-free *mst* mutant cells

The finding that mutations in *mst* suppress kinetochore-dependent MT formation, prompted us to investigate whether *Drosophila* cells lacking both chromosome- and centrosome-driven MTs manage to assemble a mitotic spindle. We thus constructed flies simultaneously mutant for both *mst* and *Sas-4*. Previous studies have shown that *Sas-4* is required for centriole duplication and that most cells of *Sas-4* mutant brains are devoid of centrosomes (Basto et al., 2006). Larval brains from *mst*; *Sas-4* double mutants stained for tubulin, Cnn and DNA displayed a very high mitotic index with most dividing cells arrested in metaphase with highly contracted chromosomes (Fig. 6A). The centrosome-free cells that arrested in metaphase (95% of metaphases lacked Cnn signals) displayed very peculiar 'spindles'. Examination of 455 metaphases revealed that 34% of them were devoid of MT arrays, 4% showed small and disorganized bipolar spindles, and 62% displayed acentrosomal MT arrays (AMTAs) resembling monopolar spindles. These AMTAs were always associated with the metaphase chromosomes, with some MTs terminating at the chromosomes and others extending beyond the chromosomes (Fig. 6A).

To analyze MT organization in *mst*; *Sas-4* AMTAs, we stained preparations for γ-tubulin, Asp or Mud; Asp and Mud are known to associate with the MT minus ends at the spindle poles (Bowman et al., 2006; do Carmo Avides and Glover, 1999; Izumi et al., 2006; Siller et al., 2006; Wakefield et al., 2001). Although γ-tubulin was enriched at the centrosomes of *mst* monopolar spindles, neither the poles of *mst*; *Sas-4* AMTAs nor the poles of the acentrosomal spindles of *Sas-4* mutants displayed detectable γ-tubulin accumulations (data not shown), which is consistent with previous

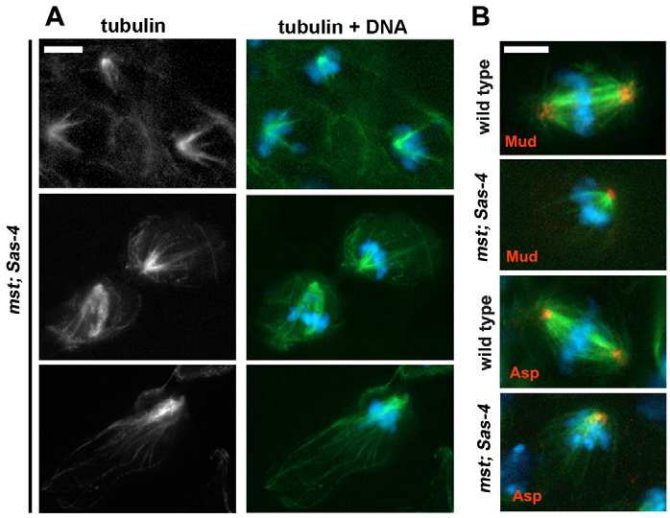

Fig. 6. *mst; Sas-4* double mutants form polarized MT arrays in mitotic cells. (**A**) *Sas-4* and *mst; Sas-4* metaphase figures stained for centrosomin (to verify the absence of centrosomes; not shown), tubulin (green) and DNA (blue). Despite the absence of centrosomes, most *mst; Sas-4* mitotic cells form peculiar polarized MT arrays that either terminate at, or extend beyond the chromosomes. (**B**) Metaphase figures from wild-type and *mst; Sas-4* brains stained for either Mud or Asp (red), tubulin (green) and DNA (blue). Scale bars: 5 μm.

results on *Sas-4* mutants (Basto et al., 2006). However, we found that the poles of the AMTAs were enriched in Asp and Mud, similarly to those of the *mst* and the *Sas-4* mutant spindles (Fig. 6B). We thus conclude that the AMTAs of *mst*; *Sas-4* double mutants contain polarized MTs with the minus ends clustered at one side of the structure.

To gain insight into the formation of the AMTAs, we comparatively examined MT regrowth after cold exposure in metaphase cells from *Sas-4* single mutants and *mst; Sas-4* double mutants. Following cold exposure (40 minutes at 0°C), brains from both mutants were returned to 25°C and fixed after 2, 5 or 10 minutes. To define the MT regrowth patterns we subdivided metaphase figures into five broad categories: metaphases with no MT regrowth foci (NRF; Table 1); metaphases with MT regrowth foci (RFs) mostly associated with the chromosomes (CRFs; Fig. 7, Table 1); metaphases containing mostly chromosome-independent RFs (IRFs; Fig. 7, Table 1); metaphases with regrowing MTs forming a bipolar array (BA; Fig. 7, Table 1); metaphases with regrowing MTs forming a monopolar array (MA; Fig. 7, Table 1). After 2 minutes at 25°C, 69% of *Sas-4* mutant metaphases showed only CRFs, 14% displayed IRFs, 11% showed BAs and 6% did not exhibit RFs (NRF). By contrast, 32% of *mst; Sas-4* mutant metaphases returned at 25°C for 2 minutes displayed no RFs (NRF), 20% showed CRFs, 20% IRFs, and 28% MAs. After 5 and 10 minutes at 25°C, *Sas-4* and *mst; Sas-4* metaphases showed relative increases in bipolar (BAs) and monopolar (MAs) MT arrays, respectively (Fig. 7, Table 1). After 10 minutes at 25°C, in *Sas-4* brains 75% of metaphase figures were associated with bipolar spindles, whereas in *mst; Sas-4* brains 59% of metaphase figures were associated with monopolar MT arrays (MAs; Fig. 7, Table 1).

Together, these results indicate that the MT regrowth foci observed in *Sas-4* and in *mst; Sas-4* cells have different properties;

Table 1. Pattern of MT regrowth in *Sas-4* and *mst; Sas-4* metaphase-like cells

Mutant	Time at 25°C (minutes)	Number of cells scored	No MT regrowth foci (%)	MT regrowth foci mostly associated with chromosomes (%)	MT regrowth foci mostly not associated with chromosomes (%)	Monopolar MT arrays (%)	Bipolar MT arrays (%)
Sas-4	2	72	5.6	69.4	13.9	0	11.1
mst; Sas-4	2	71	32.4	19.7	19.7	28.2	0
Sas-4	5	408	2.9	29.4	3.4	11.8	52.5
mst; Sas-4	5	176	12.0	26.1	23.3	35.8	2.8
Sas-4	10	547	1.5	12.6	1.8	9.0	75.1
mst; Sas-4	10	85	9.4	11.8	14.1	58.8	5.9

the former give rise to bipolar spindles, whereas the latter form monopolar MT arrays. The finding that in *mst; Sas-4* mutants, the frequency of MAs increases with the time spent at 25°C and the frequency of cells with multiple MT regrowth foci concomitantly decreases, further suggests that MAs assemble from these foci, which probably coalesce to form a single monopolar structure. This hypothesis is supported by the observation of putative intermediates of this assembly process, namely cells that exhibit both an MA and additional MT regrowth foci or two incompletely fused MAs (Fig. 7).

Misato is primarily expressed during mitosis

To determine the subcellular localization of the Mst protein, we used two different anti-Mst antibodies: a commercial monoclonal antibody (Santa Cruz) and a rabbit polyclonal antibody that was generated in our laboratory. The latter antibody was raised against the entirety of Mst and affinity purified against a 3HA–Mst fusion protein (see the Materials and Methods). Western blotting analysis showed that both antibodies recognized a band of the expected size (~64 kDa) in wild-type brain extracts. In extracts from mst^{C27} and mst^{LB20} mutant brains, neither this band nor the truncated Mst forms encoded by these mutant alleles were detected (Fig. 8A). This finding supports the hypothesis that both alleles are genetically null.

Immunolocalization experiments revealed that Mst specifically accumulated in the cytoplasm of cells undergoing mitosis. Both dividing neuroblasts and GMCs displayed a strong and homogeneous Mst staining, which persisted from prophase to telophase and dramatically decreased in interphase cells**.** Immunostaining of *mst* brains did not reveal any clear signal in mitotic cells, confirming the specificity of the antibodies (Fig. 8B). Consistent with the finding that anti-Mst antibodies do not decorate the spindle MTs, Mst did not associate with MTs in sedimentation assays (supplementary material Fig. S3).

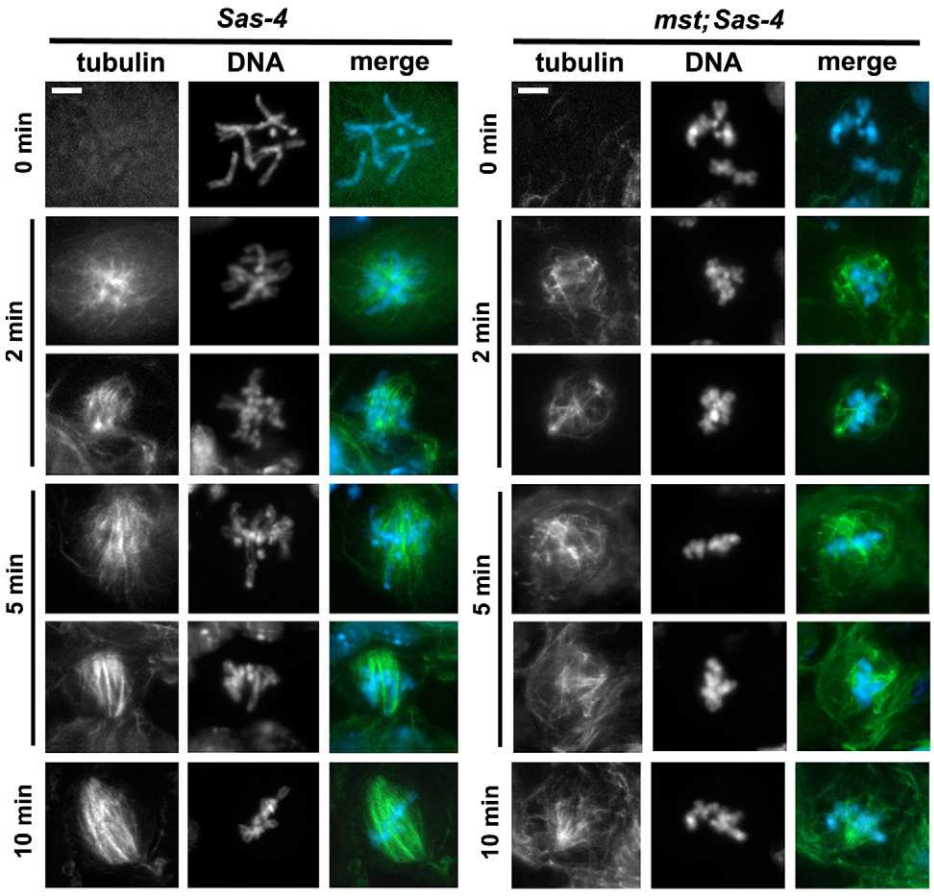

Fig. 7. MT regrowth after cold exposure in *Sas-4* and *mst; Sas-4* mutants. Cells were stained for centrosomin (to verify the absence of centrosomes; not shown), tubulin (green) and DNA (blue). In both *Sas-4* and *mst; Sas-4* brains, spindle MTs were completely depolymerized after 40 minutes of cold treatment (0 min). In most *Sas-4* cells returned at 25°C for 2 minutes, MT repolymerize almost exclusively near the chromosomes; at 5 and 10 minutes, most *Sas-4* metaphases exhibit bipolar spindles. In *mst; Sas-4* cells returned to 25°C for 2 minutes, many MT regrowth foci are distant from the chromosomes, even if they display growing MTs oriented toward the chromatin. At 5 minutes, many *mst; Sas-4* cells exhibit MT growing foci that appear to coalesce to form monopolar arrays; at 10 minutes, these monopolar arrays are well focused, resembling the AMTAs observed in non-chilled cells. Scale bars: 5 μm.

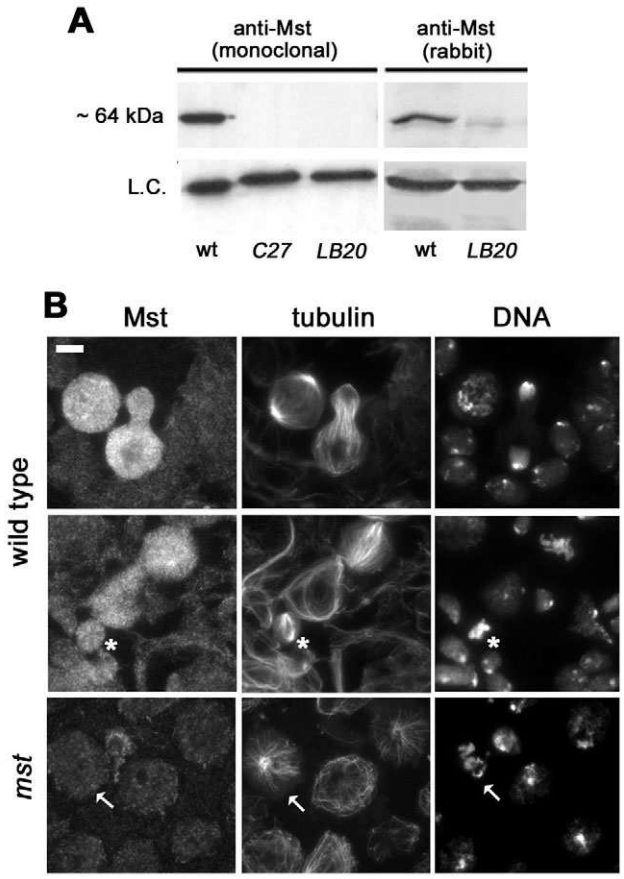

Fig. 8. Mst accumulates in mitotic cells. (**A**) Western blot of larval brain extracts from wild-type (wt), mst^{C27} and mst^{LB20} mutants. Both the monoclonal (Santa Cruz) and the polyclonal (rabbit) antibodies recognize a single band of approximately 64 kDa, which is absent in mutant brains. Giotto (Giansanti et al., 2006) was used as loading control (L.C.). (**B**) Localization of Mst in wild-type and *mst* larval brains. During mitotic division, both neuroblasts and GMCs (asterisk) exhibit a strong and diffuse Mst signal, which persists from prophase to telophase; this signal is very weak in interphase cells. Mitotic cells of *mst* mutants (arrows) do not display any staining, confirming the specificity of the antibody. Scale bar: 5 µm.

Misato is not involved in mitochondrial behavior

Studies in human cells have suggested that the Mst homologue is loosely associated with the outer mitochondrial membrane and regulates mitochondrial distribution and morphology (Kimura and Okano, 2007). We thus tested whether *Drosophila* Mst is involved in mitochondrial organization and behavior. We found that *Drosophila* Mst is not a mitochondrial component, and that mitochondria distribution in brain cells of *mst* mutants is comparable to that seen in wild-type cells (supplementary material Fig. S4 and data not shown). In addition, immunostaining with two different anti-Mst antibodies showed that Mst was not enriched in the mitochondrial derivatives (Nebenkern) of *Drosophila* spermatids (data not shown). Thus *Drosophila* Mst does not appear to be a mitochondrial component and does not affect the intracellular distribution of mitochondria.

Discussion

We have shown that *mst* function is required for chromosome-associated MT regrowth after cold exposure. Abundant evidence indicates that chromatin and kinetochores have the ability to promote MT nucleation and stabilization. Studies in *Xenopus* have shown that DNA injected into eggs promotes MT nucleation leading to the formation of spindle-like structures. Spindle-like structures were also observed around DNA-coated beads incubated in *Xenopus* egg extracts (reviewed by Karsenti and Vernos, 2001). These findings suggested that the process of spindle formation does not require the centromere–kinetochore function. However, several studies have demonstrated that in somatic cells recovering from MT poisons or cold exposure, MTs regrow from the kinetochores and not from chromosome arms (Witt et al., 1980; De Brabander et al., 1981; Tulu et al., 2006; Torosantucci et al., 2008; Bucciarelli et al., 2009; O'Connel and Khodjakov, 2007). Consistent with these results, RCC1 and other factors regulating the Ran GTP–GDP cycle are enriched at mammalian kinetochores (Bishoff et al., 1990; Joseph et al., 2004), and RanGTP accumulates at the kinetochore of cells recovering from MT depolymerization (Torosantucci et al., 2008). Most importantly, there is evidence that kinetochores can drive MT growth even under physiological conditions. Studies in mammalian cells have shown that in monopolar spindles the kinetochores that face away from the centrosome can drive formation of k-fibers (Khodjakov et al., 2003). Similarly, in *Drosophila* S2 cells, chromosomes that are distant from the astral MTs develop k-fibers from the kinetochore that does not face the centrosome (Maiato et al., 2004b). Thus, in both *Drosophila* and mammalian cells, chromosome-induced MT growth occurs primarily at the centromere–kinetochore region.

The pattern of MT regrowth observed in our experiments on wild-type neuroblasts is very similar to the pattern of kinetochore-driven formation of k-fibers observed in *Drosophila* S2 cells either untreated or exposed to MT-depolymerizing agents (Bucciarelli et al., 2009; Maiato et al., 2004b). To explain the mechanism of kinetochore-driven k-fiber formation it has been proposed that kinetochores capture the plus ends of MTs nucleated near the centromere; these MTs continue to polymerize at the kinetochore, forming MT bundles with the minus ends pointing away from the chromosomes. Interactions between these MT bundles and the astral MTs lead to the formation of mature k-fibers that connect the chromosomes with the spindle poles (Lüders et al., 2006; Maiato et al., 2004b). Our results are consistent with this model, and strongly suggest that *mst* mutants are specifically defective in kinetochore-driven but not centrosome-driven MT growth. MTs emanating from *mst* centrosomes eventually reach the kinetochores and form sparse k-fibers, which are much thinner than those of wild-type cells because they do not incorporate the MTs generated by the kinetochores (Figs 1 and 4).

The role of *mst* in kinetochore-induced MT formation is currently unknown. Studies in human cells have suggested that an Mst homologue is localized at the outer mitochondrial membrane and regulates mitochondrial distribution and morphology (Kimura and Okano, 2007). However, it is unlikely that *mst* regulates MT growth by affecting mitochondrial functions, because we found that *Drosophila* Mst is not associated with mitochondria. We also found that Mst does not associate with MTs in pull-down assays, which is consistent with the finding that anti-Mst antibodies do not decorate the spindle MTs. In addition, preliminary co-immunoprecipitation and mass spectrometry experiments did not reveal reliable Mst interactors. Thus, our data do not provide indications on whether *mst* mutants are defective in chromatin-induced MT nucleation near the centromere or in the subsequent kinetochore-driven formation of k-fibers. It is also possible that the

mst function is not restricted to the formation of k-fibers and that *mst* has functions that are general to MT behavior, such as MT dynamics or bundling. However, even if *mst* had a more general role in MT behavior, kinetochore-driven MTs are clearly more susceptible to the loss of *mst* function than are other MTs. We found that Mst is primarily expressed during mitosis, and accumulates in dividing cells from prophase through telophase. This finding leads us to speculate that Mst might be involved in the upregulation of MT dynamics that characterizes the interphase to M-phase transition. However, the molecular mechanisms underlying the Mst-dependent MT behavior and the specific role of Mst in kinetochore-driven k-fiber formation are currently unclear and remain a matter for future studies.

An incomplete occupancy of the kinetochore plate by k-MTs is probably responsible for SAC protein recruitment at kinetochores and SAC-mediated metaphase arrest in *mst* mutants (Karess, 2005; Musacchio and Salmon, 2007). When the SAC is abrogated by a mutation in the *rod* gene, a fraction of the metaphases of *mst* mutant brains manages to undergo anaphase. However, most mutant anaphases seen in *mst; rod* double mutants exhibit defects in chromosome segregation that are more severe than those observed in *rod* single mutants, suggesting that the thin k-fibers of *mst* mutant cells have a reduced ability to mediate chromosome segregation. Interestingly, *mst; rod* double mutants displayed a lower frequency of polyploid cells than *mst* single mutants. A possible interpretation for this finding is that loss of *rod* function in an *mst* mutant background releases bipolar spindles from SAC-induced metaphase arrest, allowing chromosome segregation and preventing polyploid cell formation. It can be also envisaged that in *mst; rod* double mutants, a fraction of the mitotic cells undergoes anaphase before aster collapse, further reducing polyploid cell formation.

In *mst* mutant brains, prophase cells display normal aster separation, whereas most prometaphase–metaphase figures are monopolar. This suggests that k-fibers are required to maintain aster separation after nuclear envelope breakdown (NEB). Several studies indicate that k-fibers have a role in aster separation. However, the effects of k-fiber disruption appear to be cell-type specific. The Aurora A activator TPX2 is required for both chromosome-dependent MT formation and the assembly of a bipolar spindle (Karsenti, 2005). However, there is a controversy on the spindle abnormalities caused by depletion of TPX2 in human cells. A study showed that loss of TPX2 causes centrosome fragmentation and multipolar spindles in HeLa cells (Garret et al., 2002). In other studies on HeLa cells, TPX2 depletion resulted in two prominent asters that did not interact to form a bipolar spindle (Gruss et al., 2002; Tulu et al., 2006). More recent work has shown that RNAi against *TPX2* in U2OS cells leads to aster collapse and monopolar spindles (Bird and Hyman, 2008). In *Caenorhabditis elegans* embryos depleted of the TPX2 ortholog TPXL-1, asters also collapsed, but gave rise to short bipolar spindles (Ozlü et al., 2005). Another factor required for both k-fiber formation and centrosome separation is the human kinetochore protein Mcm21R/CENP-O (McAinsh et al., 2006); recent work on this protein has led to the conclusion that k-fibers use the poleward MT flux to generate forces that push centrosomes apart (Toso et al., 2009). Analysis of *Drosophila* mitosis has provided additional evidence for a role of k-fibers in centrosome separation. The conserved *Drosophila* Orbit/Mast protein (CLASP in vertebrates) is required for tubulin dimer addition to the MT plus ends of fluxing k-fibers and for the maintenance of kinetochore and k-fiber connection (Maiato et al., 2002; Maiato et al., 2005). Mutations in *orbit/mast* and RNAi-mediated knockdown of these genes cause aster collapse and frequent monopolar spindles in embryonic and S2 tissue culture cells, respectively (Maiato et al., 2002; Maiato et al., 2005; Laycock et al., 2006). Finally, it has been observed that RNAi-mediated depletion of the augmin complex (Goshima et al., 2008) in S2 cells leads to a complete suppression of k-fiber regrowth after cold exposure (Bucciarelli et al., 2009) and to the formation of monopolar spindles (Bucciarelli et al., 2009; Goshima et al., 2007; Goshima et al., 2008; Somma et al., 2008). Collectively, these results indicate that in many systems, the fluxing MTs of k-fibers exert forces required to maintain proper spindle architecture. We propose that the thin k-fibers of *mst* mutant spindles are unable to generate sufficient force to keep the centrosomes apart and avoid aster collapse.

To the best of our knowledge, *mst* is the first *Drosophila* gene so far identified that appears to be specifically required for kinetochore-driven MT formation during mitosis of a living organism. The *orbit/mast* gene and the augmin-coding genes (*wac* and *msd1*) are not specifically involved in this process. Orbit/Mast is a microtubule-associated protein that is particularly enriched at the spindle poles and the central spindle midzone, and it is required for both spindle assembly and cytokinesis (Inoue et al., 2000; Inoue et al., 2004; Lemos et al., 2000). Studies on two augmin subunits, Wac and Msd1, have shown that they are not essential for mitotic spindle formation and fly viability, but are only required for meiotic spindle organization in females (Meireles et al., 2009; Wainman et al., 2009). Thus, the analysis of *mst* mutants allowed us to define the role of kinetochore-driven MT formation in living flies. Previous studies have shown that lack of centrosomal MTs results in anastral, but otherwise functional spindles (Basto et al., 2006; Bonaccorsi et al., 2000; Giansanti et al., 2008; Megraw et al., 2001), and there is evidence that flies without centrosomes can develop to adulthood (Basto et al., 2006). By contrast, our results indicate that kinetochore-driven MT formation is an essential process for *Drosophila* mitotic division and development.

The specific involvement of Mst in kinetochore-driven MT formation gave us the opportunity to ask whether *Drosophila* brain cells can form a spindle in the absence of both centrosomal and kinetochore-driven MTs. We found that most *mst; Sas-4* cells displayed acentrosomal MT arrays (AMTAs) that resembled monopolar spindles. MT regrowth assays showed that in *mst; Sas-4* metaphases, MTs grow from multiple foci, which eventually aggregate to form a monopolar MT array that is indistinguishable from an AMTA observed in non-chilled cells. In cells returned to 25°C for 2 minutes, we observed robust MT regrowth foci that were well separated from the chromosomes. These foci are likely to contain MTs nucleated independently of the chromosomes, perhaps by MT nucleation sites associated with membrane and/or Golgi (Kodani and Sütterlin, 2009). The same cells also contained foci that appeared to lie on or near the chromosomes (Fig. 7). However, the finding that *mst* single mutants are severely defective in chromosome-driven MT regrowth suggests that most, if not all, of the foci that appear to lie over the chromosomes (because of the squashing procedure used to obtain brain preparations) do in fact contain MTs that were nucleated independently of the chromatin.

We thus propose that in *mst; Sas-4* mutants all MT growth foci contain MTs that were nucleated independently of the chromosomes (Fig. 9); these foci would associate with the chromosomes through a RanGTP-dependent mechanism that attracts growing MTs towards the chromatin (Athale et al., 2008; Carazo-Salas and

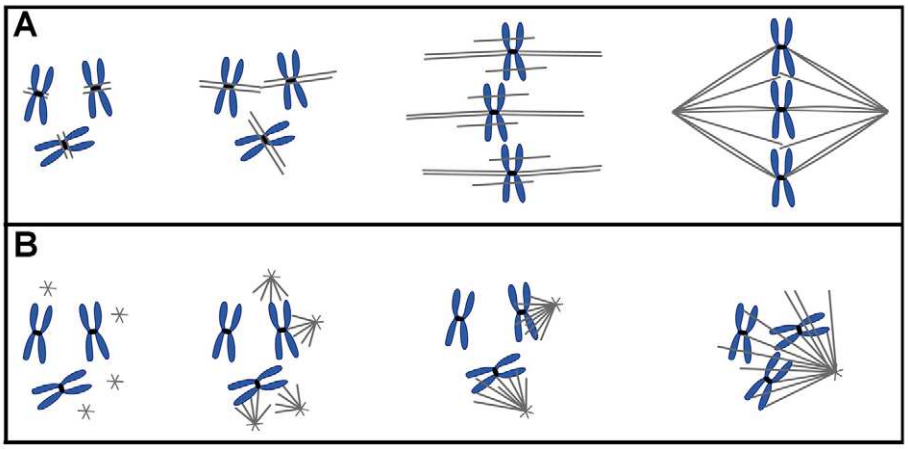

Fig. 9. Proposed model for the formation of bipolar and monopolar MT arrays in *Sas-4* and *mst; Sas-4* mutants. (**A**) In *Sas-4* mutants, kinetochores generate randomly oriented k-fibers that are progressively oriented and focused by MT-based molecular motors to form bipolar spindles. (**B**) In *mst; Sas-4* double mutants, kinetochores do not drive k-fiber formation and MTs grow from multiple foci that are distant from the chromosomes. The MTs emanating form these foci grow asymmetrically, leading to a movement of the foci toward the chromosomes. Concomitant with this movement, the foci coalesce giving rise to the AMTAs.

Karsenti, 2003; O'Connell et al., 2009). Studies using an in vitro system containing *Xenopus* egg extracts, chromatin-coated beads and purified human centrosomes have shown that the MTs nucleated by the centrosomes grow towards the chromatin. This leads to a concomitant movement of the asters, which stops when the astral MTs are stabilized by the high RanGTP concentration around the chromatin (Athale et al., 2008; Carazo-Salas and Karsenti, 2003). A Ran-GTP-mediated attraction of astral MTs has also been described in mammalian cells; mammalian chromosomes with defective kinetochores, but capable of generating a normal RanGTP gradient are unable to form k-fibers but retain the ability to attract astral MTs (O'Connell et al., 2009). We thus suggest that in an *mst* mutant background, kinetochore-driven k-fiber formation is inhibited, whereas chromosomes retain the ability to form a RanGTP gradient that attracts the MTs nucleated at either the centrosomes or other cellular sites. In the absence of centrosomes, the MTs emanating from several chromosome-independent growth foci would be attracted by the chromatin, ultimately leading to chromosome-associated AMTAs (Fig. 9).

The size of AMTAs would suggest that MTs nucleated at non-canonical sites provide a substantial contribution to mitotic spindle assembly. However, it should be considered that the relatively large size of AMTAs could be the consequence of an increase in tubulin dimer availability as a result of the inhibition of MT polymerization at both the centrosomes and chromosomes. Consistent with this view, in both *mst* and *Sas-4* single mutants, chromosome-independent MT regrowth foci were smaller and less frequent than in the double mutants. In addition, previous studies have shown that in both mammalian and *Drosophila* cells, inhibition of chromosome-dependent MT formation results in overgrowth of asters (Bucciarelli et al., 2009; Tulu et al., 2006). Collectively, these results indicate that centrosomes and kinetochores have dominant roles in mitotic MT nucleation over non-canonical nucleation sites.

Previous studies have shown that *Drosophila* cells depleted of factors required for proper spindle assembly can form short bipolar spindles (Goshima et al., 2007; Somma et al., 2008). Even if many of the AMTAs observed in *mst; Sas-4* cells comprise enough MTs to form a short bipolar spindle, in both untreated cells and cells subjected to MT regrowth, bipolar MT arrays were rare. By contrast, MT regrowth in *Sas-4* single mutants mostly generated bipolar spindles. Thus, in *Drosophila* somatic cells the assembly of both centrosomal and acentrosomal bipolar spindles requires kinetochore-driven MT formation and cannot rely on MTs nucleated in other cellular compartments.

Materials and Methods

Drosophila strains and crosses

The mst^{C27} (or mst^{3}) and mst^{LB20} (or mst^{2}) mutant alleles (Miklos et al., 1998) were kept in stocks over the X chromosome balancer *FM7*, marked with *y*, w^{a} and *B*. *mst/Y* male larvae were sorted from their *FM7/Y* sibs on the basis of the color of the Malpighian tubules. The $klp61F^{3}$ allele has been described previously (Heck et al., 1993). To construct the *mst; rod* double mutant we crossed rod^{1100}/*TM6B* males to mst^{LB20}/*FM7; e/TM6B* females. The *FM7/Y;* rod^{1100}/*TM6B* males resulting from this cross were mated to mst^{LB20}/*FM7; e/TM6B* females. The mst^{LB20}/*FM7;* rod^{1100}/*TM6B* female and *FM7/Y*; rod^{1100}/*TM6B* male progeny were then crossed to each other to obtain a stable stock. The *mst; Sas-4* double mutant was obtained by crossing mst^{LB20}/*FM7; e/TM6B* females to *FM7/Y; Sas-4/TM6B* males. The mst^{LB20}/*FM7; Sas-4/TM6B* female and *FM7/Y; Sas-4/TM6B* male progeny were then crossed to each other to obtain a stable stock. Double mutant male larvae from each stock were recognized by their yellow Malpighian tubules and non-Tubby phenotype. As controls, we used either Oregon R or *FM7/Y* males. The genetic markers and special chromosomes are described in detail in FlyBase (http://www.flybase.org).

Antibody production and western blotting

A DNA sequence encoding the entire Mst protein was first cloned in pENTER^{TM}/SD/D-TOPO (Invitrogen) and then in the expression vector pET200/D-TOPO (Invitrogen). The expressed protein was purified by SDS-PAGE, electroeluted and then used for rabbit immunization according to standard protocols. Immunization was carried out by Agro-Bio (La Ferté St Aubin, France). The crude rabbit serum was affinity purified against a 3HA–Misato fusion protein, using standard protocols. Western blotting was performed as described (Somma et al., 2002). The affinity-purified rabbit polyclonal and the monoclonal (Santa-Cruz) anti-Mst antibodies were diluted 1:1000 and 1:5000, respectively. The rabbit anti-Giotto antibody (Giansanti et al., 2006) used as loading control was diluted 1:5000.

Cytology and image analysis

DAPI-stained brain squashes were obtained according to published methods (Gatti et al., 1994). To estimate the mitotic indexes (MIs) in mutants and controls, we determined the average number of mitotic figures per optic field as described previously (Gatti and Baker, 1989).

For immunostaining experiments, brains from third instar larvae were dissected and fixed as described (Bonaccorsi et al., 2000). After several rinses in phosphate-buffered saline (PBS), brain preparations were incubated overnight at 4°C with a monoclonal anti-α-tubulin antibody (Sigma), diluted 1:1000 in PBS, and any of the following rabbit antibodies also diluted in PBS: affinity-purified anti-Misato (1:100); anti-Sea/SLC25A1 (1:100); anti-Centrosomin (1:300; gift from Tim Megraw, Florida State University, Tallahassee, FL, and Thomas Kaufman, Indiana University, Bloomington, IN); anti-γ-tubulin (1:1000, Sigma); anti-Dgrip91 (1:200; gift from Yixian Zheng, Carnegie Institute for Science, Baltimore, MD), anti-D-TACC (1:100) and anti-D-PLP (1:200; gifts from Jordan Raff, University of Oxford, Oxford, UK); anti-D-Sas4 (1:500; gift from Renata Basto, CNRS-Institut Curie, Paris, France); anti-Zw10 (1:100), anti-Cenp-meta (1:100) and anti-Ndc80 (1:100; gifts from Michael L. Goldberg, Cornell University, Ithaca, NY), anti-Incenp (1:500; gift of Mar Carmena, University of Edinburgh, Edinburgh, UK); anti-Asp (1:100) and anti Aurora B (1:200; gift from David M. Glover, University of Cambridge, Cambridge, UK); anti Cenp-C (1:200; gift from Christian Lehner, University of Zurich, Zurich, Switzerland); anti-Mud (1:200, gift from Fumio Matsuzaki, RIKEN Center for Developmental Biology, Kobe, Japan). After two rinses in PBS, primary antibodies were detected by 1 hour incubation at room temperature with FITC-conjugated anti-mouse IgG + IgM (1:20; Jackson Laboratories) and Alexa-Fluor-555-conjugated anti-rabbit IgG (1:300; Molecular Probes), diluted in PBS. The chicken anti-Cid

antibody (a gift from Gary H. Karpen, Lawrence Berkeley National Laboratory, Berkeley, CA) was diluted 1:250 and detected with Cy3-conjugated anti-chicken IgG (1:50; Jackson Laboratories). In all cases, immunostained preparations were mounted in Vectashield medium H-1200 (Vector Laboratories) containing the DNA dye DAPI (4,6 diamidino-2-phenylindole). Preparations were examined with a Zeiss Axioplan microscope, equipped with an HBO100W mercury lamp and a cooled charged-coupled device (CCD camera; Photometrics CoolSnap HQ). Grayscale images were collected separately, converted to Photoshop (Adobe Systems), pseudocolored and merged.

To estimate the MT density in wild-type metaphase half spindles and mutant monopolar spindles, the mean pixel intensities of tubulin fluorescence were measured within a fixed region using the ImageJ software (rsb.info.nih.gov/ij/). The fluorescence intensity of an area adjacent to the region of interest was used for background subtraction. We performed this analysis on half spindles and monoplar spindles of similar length, and excluded from measurements the monoplar spindle MTs that extend beyond the chromosomes.

Microtubule regrowth assays

Brains from third instar larvae were dissected in 0.7% NaCl and placed on ice for 40 minutes to depolymerize the microtubules. Brains were then placed at 25°C for 1, 2, 5 or 10 minutes, fixed according to (Bonaccorsi et al., 2000) and then immunostained for tubulin and Cnn as described above.

Mitochondrial extract analysis

Mitochondrial extracts were generated as described (Morciano et al., 2009). The quality of the extracts was checked by western blotting using an antibody against the Sea/SLC25A1 mitochondrial marker (Morciano et al., 2009) diluted 1:2000.

Microtubule sedimentation assay

Microtubule spin-down experiments were performed as described (Gergely et al., 2000; Raff et al., 1993). Briefly, 0–4 hour embryos were dechorionated, washed twice with NaCl–Triton and lysed in PEM (0.1 M PIPES, pH 6.6, 5 mM EGTA, 1 mM $MgSO_4$) with proteases inhibitors and 1 mM DTT. MTs were depolymerized by incubation in ice for 30 minutes and then centrifuged at 140,000 ***g*** for 30 minutes. MTs were polymerized by addition of taxol and GTP to the supernatant, which was kept at 25°C for 30 minutes, layered onto a 30% sucrose cushion, and centrifuged at 80,000 ***g*** for 30 minutes. In control experiments no GTP or taxol was added to the extract, and the extract was not warmed to 25°C. After centrifugation, the supernatant and the pellet were resuspended in protein sample buffer, resolved by PAGE, blotted and then probed with polyclonal anti-Mst (1:5000), anti-α-tubulin (Sigma, 1:15,000), and anti-D-TACC (1:10,000, a gift from T. Megraw).

We thank R. Basto, M. Carmena, D. Glover, M. Goldberg, G. Karpen, T. Kaufman, C. Lehner, F. Matsuzaki, T. Megraw, J. Raff and Y. Zheng for generously providing antibodies. This work was supported in part by grants from Centro di Eccellenza di Biologia e Medicina Molecolare (BEMM) to M.G., and from the Italian Association for Cancer Research (AIRC) to G.C.

Supplementary material available online at
http://jcs.biologists.org/cgi/content/full/124/5/706/DC1

References

Athale, C. A., Dinarina, A., Mora-Coral, M., Pugieux, C., Nedelec, F. and Karsenti, E. (2008). Regulation of microtubule dynamics by reaction cascades around chromosomes. *Science* **322**, 1243-1247.

Basto, R., Lau, J., Vinogradova, T., Gardiol, A., Woods, C. G., Khodjakov, A. and Raff, J. W. (2006). Flies without centrioles. *Cell* **125**, 1375-1386.

Bettencourt-Dias, M. and Glover, D. M. (2007). Centrosome biogenesis and function: centrosomics brings new understanding. *Nat. Rev. Mol. Cell Biol.* **8**, 451-463.

Bird, A. W. and Hyman, A. A. (2008). Building a spindle of the correct length in human cells requires the interaction between TPX2 and Aurora A. *J. Cell Biol.* **182**, 289-300.

Bischoff, F. R., Maier, G., Tilz, G. and Ponstingl, H. (1990). A 47-kDa human nuclear protein recognized by antikinetochore autoimmune sera is homologous with the protein encoded by RCC1, a gene implicated in onset of chromosome condensation. *Proc. Natl. Acad. Sci USA* **87**, 8617-8621.

Bonaccorsi, S., Giansanti, M. G. and Gatti, M. (2000). Spindle assembly in *Drosophila* neuroblasts and ganglion mother cells. *Nature Cell. Biol.* **2**, 54-56.

Bowman, S. K., Neumüller, R. A., Novatchkova, M., Du, Q. and Knoblich, J. A. (2006). The *Drosophila* NuMA Homolog Mud regulates spindle orientation in asymmetric cell division. *Dev. Cell* **10**, 731-742.

Bucciarelli, E., Pellacani, C., Naim, V., Palena, A., Gatti, M. and Somma, M. P. (2009). *Drosophila* Dgt6 interacts with Ndc80, Msps/XMAP215, and gamma-tubulin to promote kinetochore-driven MT formation. *Curr. Biol.* **19**, 1839-1845.

Carazo-Salas, R. E. and Karsenti, E. (2003). Long-range communication between chromatin and microtubules in *Xenopus* egg extracts. *Curr. Biol.* **13**, 1728-1733.

Casanova, C. M., Rybina, S., Yokoyama, H., Karsenti, E. and Mattaj, I. W. (2008). Hepatoma up-regulated protein is required for chromatin-induced microtubule assembly independently of TPX2. *Mol. Biol. Cell* **19**, 4900-4908.

Ciciarello, M., Mangiacasale, R. and Lavia, P. (2007). Spatial control of mitosis by the GTPase Ran. *Cell. Mol. Life Sci.* **64**, 1891-1914.

De Brabander, M., Geuens, G., De Mey, J. and Joniau, M. (1981). Nucleated assembly of mitotic microtubules in living PTK2 cells after release from nocodazole treatment. *Cell Motil.* **1**, 469-483.

do Carmo Avides, M. and Glover, D. M. (1999). Abnormal spindle protein, Asp, and the integrity of mitotic centrosomal microtubule organizing centers. *Science* **283**, 1733-1735.

Garrett, S., Auer, K., Compton, D. A. and Kapoor, T. M. (2002). hTPX2 is required for normal spindle morphology and centrosome integrity during vertebrate cell division. *Curr. Biol.* **12**, 2055-2059.

Gatti, M. and Baker, B. S. (1989). Genes controlling essential cell-cycle functions in *Drosophila melanogaster*. *Genes Dev.* **3**, 438-453.

Gatti, M. and Goldberg, M. L. (1991). Mutations affecting cell division in *Drosophila*. *Methods Cell Biol.* **35**, 543-586.

Gatti, M., Bonaccorsi, S. and Pimpinelli, S. (1994). Looking at *Drosophila* mitotic chromosomes. *Methods Cell Biol.* **44**, 371-391.

Gergely, F., Kidd, D., Jeffers, K., Wakefield, J. G. and Raff, J. W. (2000). D-TACC: a novel centrosomal protein required for normal spindle function in the early *Drosophila* embryo. *EMBO J.* **19**, 241-252.

Giansanti, M. G., Bonaccorsi, S., Kurek, R., Farkas, R. M., Dimitri, P., Fuller, M. T. and Gatti, M. (2006). The class I PITP Giotto is required for *Drosophila* cytokinesis. *Curr. Biol.* **16**, 195-201.

Giansanti, M. G., Bucciareli, E., Bonaccorsi, S. and Gatti, M. (2008). *Drosophila* SPD-2 is an essential centriole component required for PCM recruitment and astral-microtubule nucleation. *Curr. Biol.* **18**, 303-309.

Goshima, G., Wollman, R., Goodwin, S. S., Zhang, N., Scholey, J. M., Vale, R. D. and Stuurman, N. (2007). Genes required for mitotic spindle assembly in *Drosophila* S2 cells. *Science* **316**, 417-421.

Goshima, G., Mayer, M., Zhang, N., Stuurman, N. and Vale, R. D. (2008). Augmin: a protein complex required for centrosome-independent microtubule generation within the spindle. *J. Cell Biol.* **181**, 421-429.

Gruss, O. J., Wittmann, M., Yokoyama, H., Pepperkok, R., Kufer, T., Sillje, H., Karsenti, E., Mattaj, I. W. and Vernos, I. (2002). Chromosome-induced microtubule assembly mediated by TPX2 is required for spindle formation in HeLa cells. *Nat. Cell Biol.* **4**, 871-879.

Gueth-Hallonet, C., Antony, C., Aghion, J., Santa-Maria, A., Lajoie-Mazenc, I., Wright, M. and Maro, B. (1993). gamma-Tubulin is present in acentriolar MTOCs during early mouse development. *J. Cell Sci.* **105**, 157-166.

Gurvitz, A., Hartig, A., Ruis, H., Hamilton, B. and de Couet, H. G. (2002). Preliminary characterisation of DML1, an essential *Saccharomyces cerevisiae* gene related to *misato* of *Drosophila melanogaster. FEMS Yeast Res.* **2**, 123-135.

Heck, M. M., Pereira, A., Pesavento, P., Yannoni, Y., Spradling, A. C. and Goldstein, L. S. (1993). The kinesin-like protein KLP61F is essential for mitosis in *Drosophila*. *J. Cell Biol.* **123**, 665-679.

Inoue, Y. H., do Carmo Avides, M., Shiraki, M., Deak, P., Yamaguchi, M., Nishimoto, Y., Matsukage, A. and Glover, D. M. (2000). Orbit, a novel microtubule-associated protein essential for mitosis in *Drosophila melanogaster*. *J. Cell Biol.* **149**, 153-166.

Inoue, Y. H., Savoian, M. S., Suzuki, T., Máthé, E., Yamamoto, M. T. and Glover, D. M. (2004). Mutations in *orbit/mast* reveal that the central spindle is comprised of two microtubule populations, those that initiate cleavage and those that propagate furrow ingression. *J. Cell Biol.* **166**, 49-60.

Izumi, Y., Ohta, N., Hisata, K., Raabe, T. and Matsuzaki, F. (2006). *Drosophila* Pins-binding protein Mud regulates spindle-polarity coupling and centrosome organization. *Nat. Cell Biol.* **8**, 586-593.

Joseph, J., Liu, S. T., Jablonski, S. A., Yen, T. J. and Dasso, M. (2004). The RanGAP1-RanBP2 complex is essential for microtubule-kinetochore interactions in vivo. *Curr. Biol.* **14**, 611-617.

Kalab, P. and Heald, R. (2008). The RanGTP gradient-a GPS for the mitotic spindle. *J. Cell Sci.* **121**, 1577-1586.

Kallio, M. J., McCleland, M. L., Stukenberg, P. T. and Gorbsky, G. J. (2002). Inhibition of aurora B kinase blocks chromosome segregation, overrides the spindle checkpoint, and perturbs microtubule dynamics in mitosis. *Curr. Biol.* **12**, 900-905.

Karess, R. (2005). Rod-Zw10-Zwilch: a key player in the spindle checkpoint. *Trends Cell Biol.* **15**, 386-392.

Karsenti, E. (2005). TPX or not TPX? *Mol. Cell* **19**, 431-432.

Karsenti, E. and Vernos, I. (2001). The mitotic spindle: a self-made machine. *Science* **294**, 543-547.

Khodjakov, A., Cole, R. W., Oakley, B. R. and Rieder, C. L. (2000). Centrosome-independent mitotic spindle formation in vertebrates. *Curr. Biol.* **27**, 59-67.

Khodjakov, A., Copenagle, L., Gordon, M. B., Compton, D. A. and Kapoor, T. M. (2003). Minus-end capture of preformed kinetochore fibers contributes to spindle morphogenesis. *J. Cell Biol.* **160**, 671-683.

Kimura, M. and Okano, Y. (2007). Human Misato regulates mitochondrial distribution and morphology. *Exp. Cell Res.* **313**, 1393-1404.

Kirschner, M. and Mitchison, T. (1986). Beyond self-assembly: from microtubules to morphogenesis. *Cell* **45**, 329-342.

Kodani, A. and Sütterlin, C. (2009). A new function for an old organelle: microtubule nucleation at the Golgi apparatus. *EMBO J.* **28**, 995-996.

Lawo, S., Bashkurov, M., Mullin, M., Ferreria, M. G., Kittler, R., Habermann, B., Tagliaferro, A., Poser, I., Hutchins, J. R., Hegemann, B. et al. (2009). HAUS, the 8-subunit human augmin complex, regulates centrosome and spindle integrity. *Curr. Biol.* **19**, 816-826.

Laycock, J. E., Savoian, M. S. and Glover, D. M. (2006). Antagonistic activities of Klp10A and Orbit regulate spindle length, bipolarity and function in vivo. *J. Cell Sci.* **119**, 2354-2361.

Lemos, C. L., Sampaio, P., Maiato, H., Costa, M., Omel'yanchuk, L. V., Liberal, V. and Sunkel, C. E. (2000). Mast, a conserved microtubule-associated protein required for bipolar mitotic spindle organization. *EMBO J.* **19**, 3668-3682.

Li, K. and Kaufman, T. C. (1996). The homeotic target gene centrosomin encodes an essential centrosomal component. *Cell* **85**, 585-596.

Lüders, J. and Stearns, T. (2007). Microtubule-organizing centres: a re-evaluation. *Nat. Rev. Mol. Cell Biol.* **8**, 161-167.

Lüders, J., Patel, U. K. and Stearns, T. (2006). GCP-WD is a gamma-tubulin targeting factor required for centrosomal and chromatin-mediated microtubule nucleation. *Nat. Cell Biol.* **8**, 137-147.

Mahoney, N. M., Goshima, G., Douglass, A. D. and Vale, R. D. (2006). Making microtubules and mitotic spindles in cells without functional centrosomes. *Curr. Biol.* **16**, 564-569.

Maiato, H., Sampaio, P., Lemos, C. L., Findlay, J., Carmena, M., Earnshaw, W. C. and Sunkel, C. E. (2002). MAST/Orbit has a role in microtubule-kinetochore attachment and is essential for chromosome alignment and maintenance of spindle bipolarity. *J. Cell Biol.* **157**, 749-760.

Maiato, H., DeLuca, J., Salmon, E. D. and Earnshaw, W. C. (2004a). The dynamic kinetochore-microtubule interface. *J. Cell Sci.* **117**, 5461-5477.

Maiato, H., Rieder, C. L. and Khodjakov, A. (2004b). Kinetochore-driven formation of kinetochore fibers contributes to spindle assembly during animal mitosis. *J. Cell Biol.* **167**, 831-840.

Maiato, H., Khodjakov, A. and Rieder, C. L. (2005). *Drosophila* CLASP is required for the incorporation of microtubule subunits into fluxing kinetochore fibres. *Nat. Cell Biol.* **7**, 42-47.

McAinsh, A. D., Meraldi, P., Draviam, V. M., Toso, A. and Sorger, P. K. (2006). The human kinetochore proteins Nnf1R and Mcm21R are required for accurate chromosome segregation. *EMBO J.* **25**, 4033-4049.

Megraw, T. L., Kao, L. R. and Kaufman, T. C. (2001). Zygotic development without functional mitotic centrosomes. *Curr. Biol.* **11**, 116-120.

Meireles, A. M., Fisher, K. H., Colombie, N., Wakefield, J. G. and Ohkura, H. (2009). Wac: a new Augmin subunit required for chromosome alignment but not for acentrosomal microtubule assembly in female meiosis. *J. Cell Biol.* **184**, 777-784.

Miklos, G. L., Yamamoto, M., Burns, R. G. and Maleszka, R. (1998). An essential cell division gene of *Drosophila*, absent from *Saccharomyces,* encodes an unusual protein with tubulin-like and myosin-like peptide motifs. *Proc. Natl. Acad. Sci. USA* **94**, 5189-5194.

Mishra, R. K., Chakraborty, P., Arnaoutov, A., Fontoura, B. M. and Dasso, M. (2010). The Nup107-160 complex and gamma-TuRC regulate microtubule polymerization at kinetochores. *Nat. Cell Biol.* **12**, 164-169.

Morciano, P., Carrisi, C., Capobianco, L., Mannini, L., Burgio, G., Cestra, G., De Benedetto, G. E., Corona, D. F., Musio, A. and Cenci, G. (2009). A conserved role for the mitochondrial citrate transporter Sea/SLC25A1 in the maintenance of chromosome integrity. *Hum. Mol. Genet.* **18**, 4180-4188.

Moutinho-Pereira, S., Debec, A. and Maiato, H. (2009). Microtubule cytoskeleton remodeling by acentriolar microtubule-organizing centers at the entry and exit from mitosis in *Drosophila* somatic cells. *Mol. Biol. Cell* **20**, 2796-2808.

Musacchio, A. and Salmon, E. D. (2007). The spindle-assembly checkpoint in space and time. *Nat. Rev Mol. Cell Biol.* **8**, 379-393.

O'Connell, C. B. and Khodjakov, A. L. (2007). Cooperative mechanisms of mitotic spindle formation. *J. Cell Sci.* **120**, 1717-1722.

O'Connell, C. B., Loncarek, J., Kaláb, P. and Khodjakov, A. (2009). Relative contributions of chromatin and kinetochores to mtotic spindle assembly. *J. Cell Biol.* **187**, 43-51.

Ozlü, N., Srayko, M., Kinoshita, K., Habermann, B., O'Toole, E. T., Müller-Reichert, T., Schmalz, N., Desai, A. and Hyman, A. A. (2005). An essential function of the *C. elegans* ortholog of TPX2 is to localize activated aurora A kinase to mitotic spindles. *Dev. Cell* **9**, 237-248.

Palacios, M. J., Joshi, H. C., Simerly, C. and Schatten, G. (1993). Gamma-tubulin reorganization during mouse fertilization and early development. *J. Cell Sci.* **104**, 383-389.

Przewloka, M. R., Zhang, W., Costa, P., Archambault, V., D'Avino, P. P., Lilley, K. S., Laue, E. D., McAinsh, A. D. and Glover, D. M. (2007). Molecular analysis of core kinetochore composition and assembly in *Drosophila melanogaster. PLoS ONE* **2**, e478.

Raff, J. W., Kellogg, D. R. and Alberts, B. M. (1993). *Drosophila* gamma-tubulin is part of a complex containing two previously identified centrosomal MAPs. *J. Cell Biol.* **121**, 823-835.

Rebollo, E., Llamazares, S., Reina, J. and Gonzalez, C. (2004). Contribution of noncentrosomal microtubules to spindle assembly in *Drosophila* spermatocytes. *PLoS Biol.* **2**, E8. doi:10. 1371.

Rebollo, E., Sampaio, P., Januschke, J., Llamazares, S., Varmark, H. and González, C. (2007). Functionally unequal centrosomes drive spindle orientation in asymmetrically dividing *Drosophila* neural stem cells. *Dev. Cell* **12**, 467-474.

Rusan, N. M. and Peifer, M. (2007). A role for a novel centrosome cycle in asymmetric cell division. *J. Cell Biol.* **177**, 13-20.

Sampath, S. C., Ohi, R., Leismann, O., Salic, A., Pozniakovski, A. and Funabiki, H. (2004). The chromosomal passenger complex is required for chromatin-induced microtubule stabilization and spindle assembly. *Cell* **118**, 187-202.

Schittenhelm, R. B., Heeger, S., Althoff, F., Walter, A., Heidmann, S., Mechtler, K. and Lehner, C. F. (2007). Spatial organization of a ubiquitous eukaryotic kinetochore protein network in *Drosophila* chromosomes. *Chromosoma* **116**, 385-402.

Schuh, M. and Ellenberg, J. (2007). Self-organization of MTOCs replaces centrosome function during acentrosomal spindle assembly in live mouse oocytes. *Cell* **130**, 484-498.

Siller, K. H., Cabernard, C. and Doe, C. Q. (2006). The NuMA-related Mud protein binds Pins and regulates spindle orientation in *Drosophila* neuroblasts. *Nat. Cell Biol.* **8**, 594-600.

Somma, M. P., Fasulo, B., Cenci, G., Cundari, E. and Gatti, M. (2002). Molecular dissection of cytokinesis by RNA interference in Drosophila cultured cells. *Mol. Biol. Cell* **13**, 2448-2460.

Somma, M. P., Ceprani, F., Bucciarelli, E., Naim, V., De Arcangelis, V., Piergentili, R., Palena, A., Ciapponi, L., Giansanti, M. G., Pellacani, C. et al. (2008). Identification of *Drosophila* mitotic genes by combining co-expression analysis and RNA interference. *PLoS Genet.* **4**, e1000126.

Torosantucci, L., De Luca, M., Guarguaglini, G., Lavia, P. and Degrassi, F. (2008). Localized RanGTP accumulation promotes microtubule nucleation at kinetochores in somatic mammalian cells. *Mol. Biol. Cell* **19**, 1873-1882.

Toso, A., Winter, J. R., Garrod, A. J., Amaro, A. C., Meraldi, P. and McAinsh, A. D. (2009). Kinetochore-generated pushing forces separate centrosomes during bipolar spindle assembly. *J. Cell Biol.* **184**, 365-372.

Tulu, U. S., Fagerstrom, C., Ferenz, N. P. and Wadsworth, P. (2006). Molecular requirements for kinetochore-associated microtubule formation in mammalian cells. *Curr. Biol.* **16**, 536-541.

Uehara, R., Nozawa, R. S., Tomioka, A., Petry, S., Vale, R. D., Obuse, C. and Goshima, G. (2009). The augmin complex plays a critical role in spindle microtubule generation for mitotic progression and cytokinesis in human cells. *Proc. Natl. Acad. Sci. USA* **106**, 6998-7003.

Wainman, A., Buster, D. W., Duncan, T., Metz, J., Ma, A., Sharp, D. and Wakefield, J. G. (2009). A new Augmin subunit, Msd1, demonstrates the importance of mitotic spindle-templated microtubule nucleation in the absence of functioning centrosomes. *Genes Dev.*. **23**, 1876-1881.

Wakefield, J. G., Bonaccorsi, S. and Gatti, M. (2001). The *Drosophila* protein Asp is involved in microtubule organization during spindle formation and cytokinesis. *J. Cell Biol.* **153**, 637-648.

Walczak, C. E. and Heald, R. (2008). Mechanisms of mitotic spindle assembly and function. *Int. Rev. Cytol.* **265**, 111-158.

Williams, B. C., Karr, T. L., Montgomery, J. M. and Goldberg, M. L. (1992). The *Drosophila l(1)zw10* gene product, required for accurate mitotic chromosome segregation, is redistributed at anaphase onset. *J. Cell Biol.* **118**, 759-773.

Witt, P. L., Ris, H. and Borisy, G. G. (1980). Origin of kinetochore microtubules in Chinese hamster ovary cells. *Chromosoma* **81**, 483-505.

Zhu, H., Coppinger, J. A., Jang, C. Y., Yates, J. R., 3rd and Fang, G. (2008). FAM29A promotes microtubule amplification via recruitment of the NEDD1-gamma-tubulin complex to the mitotic spindle. *J. Cell Biol.* **183**, 835-848.

Journal of Cell Science